

On the Properties of Solutions of the Adjoint Euler Equations

Michael B. Giles Niles A. Pierce
Oxford University Computing Laboratory

Abstract

The behavior of analytic and numerical adjoint solutions is examined for the quasi-1D Euler equations. For shocked flow, the derivation of the adjoint problem reveals that the adjoint variables are continuous with zero gradient at the shock and that an internal adjoint boundary condition is required at the shock. A Green's function approach is used to derive the analytic adjoint solutions corresponding to isentropic and shocked transonic flow, revealing a logarithmic singularity at the sonic throat and confirming the expected properties at the shock. Numerical solutions obtained using both discrete and continuous adjoint formulations reveal that there is no need to explicitly enforce the adjoint shock boundary condition. Adjoint methods are demonstrated to play an important role in the error estimation of integrated quantities such as lift and drag.

1 Introduction

Adjoint problems arise naturally in the formulation of methods for optimal aerodynamic design and optimal error control. For design applications, the adjoint solution provides the linear sensitivities of an objective function such as lift or drag to a number of design variables which parameterise the shape. These sensitivities can then be used to drive an optimisation procedure. Considerable effort has been dedicated to the development of optimal design methods based on this approach [1–8]. More recently, adjoint methods have been recognised as a means of achieving error control in fluid dynamics simulations [9–12]. In this context, the adjoint solution relates the sensitivity of the objective function to the local truncation errors in the flow discretisation. This information can then be used to provide an *a posteriori* error estimate or to guide an adaptive meshing algorithm.

While significant effort has been dedicated to developing practical methods based on adjoint formulations, there has been little discussion of the properties of the adjoint solutions themselves [13]. The present work investigates various issues concerning the derivation and approximation of solutions to the quasi-1D adjoint Euler equations. The standard Lagrange multiplier derivation of Jameson [1] is extended to include the effect of shocks in the formulation of the analytic adjoint equations. Explicit inclusion of the steady Rankine–Hugoniot conditions via an additional Lagrange multiplier demonstrates that at the shock, the adjoint variables are continuous and that an internal adjoint boundary condition is required. This is consistent with a characteristic viewpoint which indicates that one internal adjoint b.c. is needed due to the disparity in the number of adjoint characteristics entering and leaving the shock. However, the conclusions differ from those of previous investigators [14–16].

The discrete adjoint equations can be formulated in two ways, either by discretising the analytic adjoint equations (the so-called ‘continuous’ approach) [1], or by transposing the discrete equations obtained by linearising the discretised flow equations (the ‘discrete’ approach)

[7]. Giles has previously shown that for quasi-1D flows with shocks, a conservative discretisation which is second-order accurate in smooth regions of the flow produces a second-order accurate approximation to the ‘lift’ integral [17]. Hence, the linearisation of such a method (on which the discrete adjoint is based) must produce a linearised lift perturbation which is at least first-order accurate. On the other hand, it is less clear whether the discretisation of the analytic adjoint equations leads to the correct adjoint solution if there is no explicit enforcement of the special shock condition.

To investigate this point, the paper derives the analytic solution to the adjoint equations for shocked flow. This is accomplished by constructing the Green’s functions for the linearised Euler equations, including the linearised Rankine–Hugoniot conditions, using an extension of the approach developed by Giles and Pierce for shock-free quasi-1D flows [13]. The analytic results compare very well with numerical results obtained using both the continuous and discrete approaches. To understand why the continuous approach behaves correctly without explicit enforcement of the adjoint shock boundary condition, a shooting method was used to march the solution back from the exit across the shock. Disregarding the adjoint shock b.c., but maintaining continuity at the shock, leads to a family of solutions of the adjoint equations. Of these, it appears that the continuous approach selects the smoothest member of the family, which corresponds to the analytic solution.

The final section of the paper discusses the use of adjoint solutions for error analysis. The error in the lift integral is shown to be an inner product of the the adjoint flow variables and the truncation error of the discretisation of the Euler equations. Estimating the truncation error gives a method of accurately estimating the error in the lift integral. With a first-order discretisation of the Euler equations, it is shown that the error estimate can be used to correct the computed value of the lift integral and obtain second-order accuracy. Alternatively, the error estimate could be used in the future as the basis for optimal grid adaptation [12].

2 Adjoint problem formulation

The quasi-1D Euler equations for steady flow in a duct of cross-section $h(x)$, on the interval $-1 \leq x \leq 1$, may be written as

$$R(U, h) \equiv \frac{d}{dx}(hF) - \frac{dh}{dx}P = 0,$$

where

$$U = \begin{pmatrix} \rho \\ \rho q \\ \rho E \end{pmatrix}, \quad F = \begin{pmatrix} \rho q \\ \rho q^2 + p \\ \rho q H \end{pmatrix}, \quad P = \begin{pmatrix} 0 \\ p \\ 0 \end{pmatrix}.$$

If the solution contains a shock at x_s , the Rankine-Hugoniot jump condition

$$[F]_{x_s^-}^{x_s^+} = 0$$

connects the smooth solutions on either side.

For design applications, linearisation of R with respect to perturbations in the flow solution u and the geometry \tilde{h} produces

$$\tilde{R} \equiv Lu - f = \left(\frac{d}{dx}(hAu) - \frac{dh}{dx}Bu \right) - \left(\frac{d\tilde{h}}{dx}P - \frac{d}{dx}(\tilde{h}F) \right) = 0, \quad (2.1)$$

where $A = (\partial F/\partial U)$ and $B = (\partial P/\partial U)$. For error analysis applications, we shall subsequently see that f is instead the truncation error.

If the objective function of interest is the ‘lift’

$$J = \int_{-1}^1 p \, dx = \int_{-1}^{x_s} p \, dx + \int_{x_s}^1 p \, dx,$$

the lift perturbation is then

$$I = \int_{-1}^{x_s} g^T u \, dx + \int_{x_s}^1 g^T u \, dx - [p]_{x_s^-}^{x_s^+} \delta, \quad (2.2)$$

where $g = (\partial p / \partial U)^T$, and the third term includes the effect of a linearised displacement in the shock location δ .

Using continuous Lagrange multipliers v to enforce the differential flow constraints on either side of the shock, and a Lagrange multiplier v_s to enforce the Rankine–Hugoniot conditions at the shock, the augmented nonlinear objective function is

$$J = \int_{-1}^{x_s} p \, dx + \int_{x_s}^1 p \, dx - \int_{-1}^{x_s} v^T R \, dx - \int_{x_s}^1 v^T R \, dx - h_s v_s^T [F]_{x_s^-}^{x_s^+},$$

where $h_s \equiv h(x_s)$. Linearising this with respect to perturbations in the geometry \tilde{h} , the shock location δ and the flow solution u gives

$$\begin{aligned} I &= \int_{-1}^{x_s} g^T u \, dx + \int_{x_s}^1 g^T u \, dx - [p]_{x_s^-}^{x_s^+} \delta \\ &\quad - \int_{-1}^{x_s} v^T (Lu - f) \, dx - \int_{x_s}^1 v^T (Lu - f) \, dx \\ &\quad - h_s v_s^T [Au]_{x_s^-}^{x_s^+} - h_s v_s^T \left[\frac{dF}{dx} \right]_{x_s^-}^{x_s^+} \delta. \end{aligned}$$

After integration by parts and rearrangement, this yields

$$\begin{aligned} I &= \int_{-1}^{x_s} v^T f \, dx + \int_{x_s}^1 v^T f \, dx \\ &\quad - \int_{-1}^{x_s} (L^* v - g)^T u \, dx - \int_{x_s}^1 (L^* v - g)^T u \, dx \\ &\quad - \delta \left(h_s v_s^T \left[\frac{dF}{dx} \right]_{x_s^-}^{x_s^+} + [p]_{x_s^-}^{x_s^+} \right) \\ &\quad - h_s (v_s - v(x_s^+))^T Au|_{x_s^+} + h_s (v_s - v(x_s^-))^T Au|_{x_s^-} \\ &\quad - [hv^T Au]_{-1}^1, \end{aligned}$$

where the adjoint operator L^* is defined by

$$L^* v \equiv -hA^T \frac{dv}{dx} - \frac{dh}{dx} B^T v.$$

The basic idea of the adjoint approach is to define the adjoint problem so as to eliminate the explicit dependence of I on u and δ , giving the adjoint form of the objective function

$$I = \int_{-1}^{x_s} v^T f \, dx + \int_{x_s}^1 v^T f \, dx = \int_{-1}^1 v^T f \, dx. \quad (2.3)$$

To eliminate the dependence on u , v must satisfy the adjoint o.d.e.

$$L^*v - g = 0, \quad (2.4)$$

and at the shock v and v_s must satisfy

$$v(x_s^-) = v_s = v(x_s^+),$$

proving that the adjoint variables are continuous across the shock. Removing the dependence of I on δ then requires that

$$h_s v^T(x_s) \left[\frac{dF}{dx} \right]_{x_s^-}^{x_s^+} = - [p]_{x_s^-}^{x_s^+},$$

which is an internal boundary condition at the shock. Noting that

$$\left[\frac{dF}{dx} \right]_{x_s^-}^{x_s^+} = \left[\frac{1}{h} \frac{dh}{dx} P \right]_{x_s^-}^{x_s^+},$$

this reduces to the simple b.c.

$$v_2(x_s) = - \left(\frac{dh}{dx}(x_s) \right)^{-1}. \quad (2.5)$$

Finally, the inlet and exit boundary conditions for the adjoint problem are defined so as to remove the explicit dependence of

$$[h v^T A u]_{-1}^1$$

on u . At a boundary where the flow equations have n incoming characteristics, and hence n imposed boundary conditions, the adjoint equations will thus have $(3-n)$ b.c.'s corresponding to an equal number of incoming adjoint characteristics [13].

The duality of the flow (primal) and adjoint (dual) problems is evident from the fact that the inhomogeneous term f in the primal problem (2.1) enters the functional in the dual problem (2.3), and correspondingly, the inhomogeneous term g in the dual problem (2.4) appears in the functional of the primal problem (2.2). The advantage of the adjoint formulation of the objective function in the context of design optimisation is that each design variable produces a different linear source term f , but the corresponding adjoint solution remains unchanged as it depends only on the choice of objective function. Therefore, the evaluation of I requires just one flow calculation and one adjoint calculation, and is relatively independent of the number of design variables [1].

A final observation is that the adjoint equation (2.4) and the adjoint shock b.c. (2.5) together cause the gradient of the adjoint variables to vanish at the shock. This may be seen by writing (2.4) using Jacobians based on the non-conservative flow variables $U_p = (\rho, q, p)^T$, so that the adjoint equation becomes,

$$h \begin{pmatrix} q & q^2 & \frac{1}{2}q^3 \\ \rho & 2\rho q & \frac{\gamma}{\gamma-1}p + \frac{3}{2}\rho q^2 \\ 0 & 1 & \frac{\gamma}{\gamma-1}q \end{pmatrix} \frac{dv}{dx} = - \begin{pmatrix} 0 \\ 0 \\ 1 + \frac{dh}{dx}v_2 \end{pmatrix},$$

and the adjoint shock b.c. produces $(dv/dx) = 0$ at the shock.

3 Analytic adjoint solutions

3.1 Outline of approach

To verify the properties of the adjoint solutions and to provide a reference for comparison with numerical results, the analytic adjoint solutions are now derived for both isentropic and shocked transonic flows.

The derivation uses a Green's function approach [13] in which we consider the linearised problem with point source terms

$$Lu_j(x, \xi) = f_j(\xi)\delta(x - \xi), \quad (3.1)$$

where $\delta(x)$ is the Dirac delta function. Using the adjoint form of the objective function (2.3), the corresponding linearised objective is

$$I_j(\xi) = \int_{-1}^1 v^T(x) f_j(\xi) \delta(x - \xi) dx = v^T(\xi) f_j(\xi).$$

Given three linearly independent vectors $f_j(\xi)$, the three simultaneous equations can then be solved for the adjoint variables

$$v^T(\xi) = \left(I_1(\xi) | I_2(\xi) | I_3(\xi) \right) \left(f_1(\xi) | f_2(\xi) | f_3(\xi) \right)^{-1}. \quad (3.2)$$

The approach is then to choose $f_j(\xi)$, solve the linearised flow equations to obtain the flow perturbation $u_j(x, \xi)$ and the shock displacement δ , evaluate $I_j(\xi)$ using (2.2) and finally obtain $v(\xi)$ from (3.2).

3.2 Isentropic transonic flow

The key to carrying out the procedure described above is to choose a set of source vectors $f_j(\xi)$ which lead to relatively simple solutions to the linearised flow equations. We begin by considering isentropic flow through a converging-diverging duct with inlet, throat and outlet located at $x = -1, 0, +1$, respectively. The nonlinear equations ensure that mass flux $mh \equiv \rho qh$, stagnation enthalpy H and stagnation pressure p_0 all remain constant along the duct. Therefore, solutions to the linear homogeneous equations must introduce uniform perturbations to these three quantities. The general solution to the linear homogeneous equations may then be written in the form

$$u(x) = \frac{a}{h(x)} \frac{\partial U}{\partial m}(x) \Big|_{H, p_0} + b \frac{\partial U}{\partial H}(x) \Big|_{p_0, M} + c \frac{\partial U}{\partial p_0}(x) \Big|_{H, M},$$

where the three vectors are linearly independent and a , b and c represent the uniform perturbations to mh , H and p_0 . To simplify the analysis, perturbations to stagnation enthalpy and pressure are introduced at fixed Mach number rather than at fixed mass flux, so that b and c both imply an additional uniform perturbation to mh . By contrast, a does not perturb either H or p_0 .

If we now consider the inhomogeneous equations with source terms $f_j(\xi)\delta(x - \xi)$, the corresponding solutions

$$u_j(x, \xi) = a(x, \xi) \frac{1}{h(x)} \frac{\partial U}{\partial m}(x) \Big|_{H, p_0} + b(x, \xi) \frac{\partial U}{\partial H}(x) \Big|_{p_0, M} + c(x, \xi) \frac{\partial U}{\partial p_0}(x) \Big|_{H, M}$$

must satisfy the homogeneous equations on either side of ξ , and therefore a, b, c will have uniform values a_1, b_1, c_1 for $x < \xi$ and a_2, b_2, c_2 for $x > \xi$. The jump conditions for the constants are obtained by integrating the dominant terms in (3.1) from $x = \xi^-$ to $x = \xi^+$, giving

$$h(\xi) \left((a_2 - a_1) \frac{1}{h(\xi)} \frac{\partial F}{\partial m}(\xi) \Big|_{H, p_0} + (b_2 - b_1) \frac{\partial F}{\partial H}(\xi) \Big|_{p_0, M} + (c_2 - c_1) \frac{\partial F}{\partial p_0}(\xi) \Big|_{H, M} \right) = f_j(\xi).$$

This jump condition suggests that by choosing the three linearly independent source vectors

$$\begin{aligned} f_1(\xi) &= \frac{h(\xi)}{h(\xi)} \frac{\partial F}{\partial m}(\xi) \Big|_{H, p_0} = \begin{pmatrix} 1 \\ q \\ H \end{pmatrix}, \\ f_2(\xi) &= h(\xi) \frac{\partial F}{\partial H}(\xi) \Big|_{p_0, M} = h(\xi) \begin{pmatrix} \frac{-\rho q}{2H} \\ 0 \\ \frac{\rho q}{2} \end{pmatrix}, \\ f_3(\xi) &= h(\xi) \frac{\partial F}{\partial p_0}(\xi) \Big|_{H, M} = \frac{h(\xi)}{p_0} \begin{pmatrix} \rho q \\ \rho q^2 + p \\ \rho q H \end{pmatrix}, \end{aligned}$$

the perturbations will have the simple properties

$$\begin{aligned} f_1(\xi) &\Rightarrow a_2 - a_1 = 1, & b_2 &= b_1, & c_2 &= c_1, \\ f_2(\xi) &\Rightarrow b_2 - b_1 = 1, & c_2 &= c_1, & a_2 &= a_1, \\ f_3(\xi) &\Rightarrow c_2 - c_1 = 1, & a_2 &= a_1, & b_2 &= b_1. \end{aligned} \tag{3.3}$$

For each source vector $f_j(\xi)$, the three remaining unknowns in the corresponding solution $u_j(x, \xi)$ are determined by the three homogeneous boundary conditions appropriate to the Mach regime under consideration. These homogeneous boundary conditions are equivalent to demanding that there is no perturbation to the boundary conditions for the original nonlinear problem.

For isentropic transonic flow, there are two boundary conditions on H and p_0 at the subsonic inlet and no boundary conditions at the supersonic exit. The third requirement is that the Mach number remains unity at the throat.

3.2.1 Change in mh at fixed H, p_0

For f_1 , the inlet boundary conditions ensure that $b = c = 0$ and the throat condition requires that a equals zero at the throat. Therefore, $a_2 = 0$ for $\xi < 0$ and $a_1 = 0$ for $\xi > 0$, leading to the solution

$$u_1(x, \xi) = \begin{cases} -\mathcal{H}(\xi - x) \frac{1}{h(x)} \frac{\partial U}{\partial m}(x) \Big|_{H, p_0}, & \xi < 0, \\ \mathcal{H}(x - \xi) \frac{1}{h(x)} \frac{\partial U}{\partial m}(x) \Big|_{H, p_0}, & \xi > 0. \end{cases}$$

Hence, if $\xi < 0$, the mass flux upstream of $x = \xi$ is reduced by a unit amount, whereas if $\xi > 0$, the mass flux downstream of $x = \xi$ is increased by a unit amount.

The objective function is

$$I_1(\xi) = \begin{cases} - \int_{-1}^{\xi} \frac{1}{h(x)} \frac{\partial p}{\partial m}(x) \Big|_{H,p_0} dx, & \xi < 0, \\ \int_{\xi}^1 \frac{1}{h(x)} \frac{\partial p}{\partial m}(x) \Big|_{H,p_0} dx, & \xi > 0. \end{cases} \quad (3.4)$$

Since

$$\frac{\partial p}{\partial m}(x) \Big|_{H,p_0} = \frac{-q}{1 - M^2},$$

and M is linear through a choked throat, then

$$\frac{\partial p}{\partial m}(x) \Big|_{H,p_0} \sim \frac{1}{x}, \quad \text{as } x \rightarrow 0.$$

It follows that

$$I_1(\xi) \sim \log(\xi), \quad \text{as } \xi \rightarrow 0,$$

so there is a logarithmic singularity in the adjoint variables at a sonic throat.

3.2.2 Change in H at fixed p_0, M

In this case, the inlet conditions on H and p_0 require $b_1 = c = 0$ and the throat condition gives $a = 0$. The solution is then

$$u_2(x, \xi) = \mathcal{H}(x - \xi) \frac{\partial U}{\partial H}(x) \Big|_{p_0, M},$$

and the corresponding objective function, $I_2(\xi)$, is zero because $\frac{\partial p}{\partial H}(x) \Big|_{p_0, M} = 0$.

3.2.3 Change in p_0 at fixed H, M

Now, the inlet conditions on H and p_0 yield $b = c_1 = 0$, and the Mach number is fixed at the throat, so again $a = 0$. The solution and linear functional thus become

$$u_3(x, \xi) = \mathcal{H}(x - \xi) \frac{\partial U}{\partial p_0}(x) \Big|_{H, M}, \quad I_3(\xi) = \int_{\xi}^1 \frac{\partial p}{\partial p_0}(x) \Big|_{H, M} dx.$$

3.2.4 Sample solution

The analytic objective functions $I(\xi)$ and adjoint solutions $v(\xi)$ corresponding to isentropic transonic flow are shown in Fig. 1. The logarithmic singularity in I_2 at the throat is reflected in the singularities of all three adjoint variables.

3.3 Shocked flow

For shocked flow, there are two boundary conditions on H and p_0 at the subsonic inlet and one boundary condition on p at the subsonic exit. The nonlinear equations once again ensure constant mass flux and stagnation enthalpy throughout the duct, but the stagnation pressure now has different constant values on either side of the shock. Consequently, solutions to the linearized equations must now admit different but constant stagnation pressure perturbations

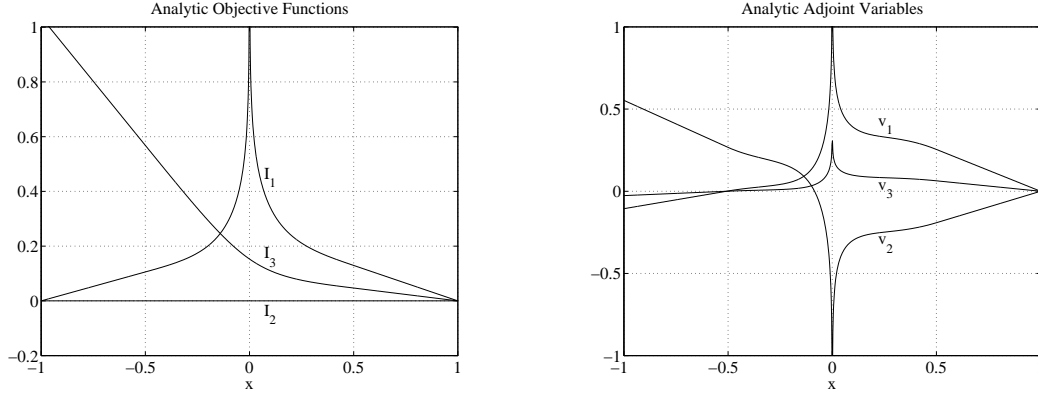


Figure 1: Objective functions and adjoint variables for isentropic transonic flow conditions.

on either side of the shock. To account for the shock, the form of the solution must be generalised to

$$u_j(x, x_s, \xi) = a(x, x_s, \xi) \frac{1}{h(x)} \frac{\partial U}{\partial m}(x) \Big|_{H, p_0} + b(x, x_s, \xi) \frac{\partial U}{\partial H}(x) \Big|_{p_0, M} + c(x, x_s, \xi) \frac{\partial U}{\partial p_0}(x) \Big|_{H, M}$$

where the perturbations a , b , and c may now be discontinuous at the shock location x_s as well as at ξ .

3.3.1 Shock movement

The displacement in the shock can be calculated from the normal shock relation

$$p_{02} = p_{01} f(M_1), \quad f(M_1) = \left(\frac{p_2}{p_1} \right) \left(\frac{1 + \frac{\gamma-1}{2} M_2^2}{1 + \frac{\gamma-1}{2} M_1^2} \right)^{\gamma/\gamma-1},$$

with shock jump conditions

$$\frac{p_2}{p_1} = 1 + \frac{2\gamma}{\gamma+1} (M_1^2 - 1), \quad M_2^2 = \frac{1 + [(\gamma-1)/2] M_1^2}{\gamma M_1^2 - (\gamma-1)/2},$$

where the subscripts 1 and 2 represent quantities upstream and downstream of the shock, respectively. The perturbations to the stagnation pressure then satisfy

$$c_2 = c_1 f(M_1) + p_{01} f'(M_1) \left(\frac{\partial M_1}{\partial x} \delta + \frac{a_1}{h(x)} \frac{\partial M_1}{\partial m}(x) \Big|_{H, p_0} \right) \Big|_{x=x_s^-}, \quad (3.5)$$

where δ is the resulting displacement of the shock and

$$\frac{\partial M}{\partial m}(x) \Big|_{H, p_0} = \frac{M}{m} \left(\frac{1 + [(\gamma-1)/2] M^2}{1 - M^2} \right).$$

If $h(x)$ is a piecewise differentiable function, then $\partial M/\partial x$ may be evaluated analytically using the area Mach number relation

$$\left(\frac{h}{h^*} \right)^2 = \frac{1}{M^2} \left[\frac{2}{\gamma+1} \left(1 + \frac{\gamma-1}{2} M^2 \right) \right]^{(\gamma+1)/(\gamma-1)}.$$

The throat is sonic so the sonic area h^* is identically equal to the throat area h_t .

3.3.2 Change in mh at fixed H, p_0

Perturbation between the inlet and the throat ($-1 < \xi < 0$)

Since the throat is choked and H and p_0 are fixed at the inlet, the form of the solution and objective function will be the same as for the isentropic transonic case when $\xi < 0$

$$u_1(x, x_s, \xi) = -\mathcal{H}(\xi - x) \frac{1}{h(x)} \frac{\partial U}{\partial m}(x) \Big|_{H, p_0}, \quad I_1(\xi) = - \int_{-1}^{\xi} \frac{1}{h(x)} \frac{\partial p}{\partial m}(x) \Big|_{H, p_0} dx.$$

The two new scenarios to consider are when ξ is between the throat and the shock and between the shock and the exit. In either case, the mass flux perturbation a will cause the shock to move and the solution will need to ensure that the perturbations to mass flux and stagnation enthalpy remain constant across the shock, in addition to satisfying the exit boundary condition on pressure.

Perturbation between the throat and the shock ($0 < \xi < x_s$)

The choked condition at the throat requires that all perturbations are zero for $x < \xi$. For consistency with the shock jump subscripts, perturbations between ξ and the shock are denoted by a_1, b_1, c_1 and perturbations between the shock and the exit are denoted by a_2, b_2, c_2 . At ξ , there is a unit mass flux perturbation at constant H and p_0 , so

$$a_1 = 1, \quad b_1 = 0, \quad c_1 = 0.$$

Furthermore, H remains constant for any shock location so $b_2 = 0$. For physical consistency, the perturbation to mass flux across the shock must be constant, and so

$$a_1 = a_2 + c_2 \left(h(x) \frac{\partial m}{\partial p_0}(x) \Big|_{H, M} \right) \Big|_{x=x_s^+}.$$

Also, to avoid perturbing the exit pressure, we require

$$\left(\frac{a_2}{h(x)} \frac{\partial p}{\partial m}(x) \Big|_{H, p_0} + c_2 \frac{\partial p}{\partial p_0}(x) \Big|_{H, M} \right) \Big|_{x=1} = 0.$$

These two equations determine the two unknowns a_2 and c_2 and equation (3.5) then determines the shock movement δ . The perturbed solution is then

$$u_1(x, x_s, \xi) = \frac{1}{h(x)} [a_1 \mathcal{H}(x - \xi) + (a_2 - a_1) \mathcal{H}(x - x_s)] \frac{\partial U}{\partial m}(x) \Big|_{H, p_0} + c_2 \mathcal{H}(x - x_s) \frac{\partial U}{\partial p_0}(x) \Big|_{H, M}.$$

and the corresponding objective function is

$$I_1(\xi) = \int_{\xi}^{x_s} \frac{a_1}{h(x)} \frac{\partial p}{\partial m}(x) \Big|_{H, p_0} dx + \int_{x_s}^1 \left(\frac{a_2}{h(x)} \frac{\partial p}{\partial m}(x) \Big|_{H, p_0} + c_2 \frac{\partial p}{\partial p_0}(x) \Big|_{H, M} \right) dx - (p_2 - p_1) \delta.$$

Perturbation between the shock and the exit ($x_s < \xi < 1$)

All perturbations are now zero for $x < x_s$, so

$$a_1 = b_1 = c_1 = 0,$$

since perturbations introduced in the subsonic region following the shock cannot affect the supersonic zone except through shock movement. Perturbations between the shock and ξ are now denoted by a_2, b_2, c_2 and perturbations between ξ and the exit are denoted by a_3, b_3, c_3 .

For compatibility with the upstream flow, there must be no perturbation to H across the shock, so $b_2 = b_3 = 0$. The perturbation to the stagnation pressure must be uniform throughout the subsonic region, so $c_2 = c_3 \equiv c$. At ξ , the source term produces a unit perturbation in mass flux so

$$a_3 - a_2 = 1.$$

To match the flow upstream of the shock, there must be no mass flux perturbation on the downstream side of the shock

$$a_2 + c \left(h(x) \frac{\partial m}{\partial p_0}(x) \Big|_{H,M} \right) \Big|_{x=x_s^+} = 0.$$

Also, to ensure zero perturbation of the exit static pressure we require,

$$\left(\frac{a_3}{h(x)} \frac{\partial p}{\partial m}(x) \Big|_{H,p_0} + c \frac{\partial p}{\partial p_0}(x) \Big|_{H,M} \right) \Big|_{x=1} = 0,$$

giving three equations for the three unknowns. The perturbed solution then has the form

$$u_1(x, x_s, \xi) = \frac{1}{h(x)} [a_2 \mathcal{H}(x - x_s) + (a_3 - a_2) \mathcal{H}(x - \xi)] \frac{\partial U}{\partial m}(x) \Big|_{H,p_0} + c \mathcal{H}(x - x_s) \frac{\partial U}{\partial p_0}(x) \Big|_{H,M},$$

with objective function

$$I_1(\xi) = \int_{x_s}^{\xi} \frac{a_2}{h(x)} \frac{\partial p}{\partial m}(x) \Big|_{H,p_0} dx + \int_{\xi}^1 \frac{a_3}{h(x)} \frac{\partial p}{\partial m}(x) \Big|_{H,p_0} dx + \int_{x_s}^1 c \frac{\partial p}{\partial p_0}(x) \Big|_{H,M} dx - (p_2 - p_1) \delta.$$

3.3.3 Change in H at fixed p_0, M

Ahead of the shock, the perturbation to stagnation pressure c must be zero due to the inlet boundary condition, and the mass flux perturbation a must be zero due to the choked throat. The inlet condition on H ensures the perturbation to stagnation enthalpy is zero for $x < \xi$, and the unit jump in b at ξ will produce a constant perturbation in H across the shock, without affecting the exit condition on pressure.

There still exists that possibility that a and c are non-zero constants following the shock, balancing to produce zero mass flux perturbation at the shock

$$\left(a + c h(x) \frac{\partial m}{\partial p_0}(x) \Big|_{H,M} \right) \Big|_{x=x_s^+} = 0,$$

and zero pressure perturbation at the exit

$$\left(\frac{a}{h(x)} \frac{\partial p}{\partial m}(x) \Big|_{H,p_0} + c \frac{\partial p}{\partial p_0}(x) \Big|_{H,M} \right) \Big|_{x=1} = 0.$$

However, the determinant of this system is nonzero, so there is only the trivial solution $a = c = 0$. Hence, the solution and objective function in the shocked case have the form

$$u_2(x, x_s, \xi) = \mathcal{H}(x - \xi) \frac{\partial U}{\partial H}(x) \Big|_{p_0, M}, \quad I_2(\xi) = 0,$$

and there is no displacement of the shock.

3.3.4 Change in p_0 at fixed H, M

For shocked flow with a unit jump in stagnation pressure, the presence of the shock affects the perturbed solution for all locations of ξ . This is in contrast to the shocked case with a jump in mass flux, where the solution remained unchanged from the isentropic transonic case for $\xi < 0$. The two scenarios to consider in the present case are when ξ is between the inlet and the shock, and between the shock and the exit.

Perturbation between the inlet and the shock ($-1 < \xi < x_s$)

As in the shock-free case, there is no perturbation for $x < \xi$. Denoting the perturbations between ξ and the shock by a_1, b_1, c_1 and those after the shock by a_2, b_2, c_2 , we have by definition

$$a_1 = 0, \quad b_1 = 0, \quad c_1 = 1.$$

The perturbation to H must be constant across the shock so $b_2 = 0$. Constant mass flux perturbation at the shock requires

$$c_1 \left(h(x) \frac{\partial m}{\partial p_0}(x) \Big|_{H,M} \right) \Big|_{x=x_s^-} = a_2 + c_2 \left(h(x) \frac{\partial m}{\partial p_0}(x) \Big|_{H,M} \right) \Big|_{x=x_s^+},$$

and zero perturbation to the exit pressure is ensured by setting

$$\left(\frac{a_2}{h(x)} \frac{\partial p}{\partial m}(x) \Big|_{H,p_0} + c_2 \frac{\partial p}{\partial p_0}(x) \Big|_{H,M} \right) \Big|_{x=1} = 0,$$

providing two equations for the two unknowns. The solution then has the form

$$u_3(x, x_s, \xi) = [c_1 \mathcal{H}(x - \xi) + (c_2 - c_1) \mathcal{H}(x - x_s)] \frac{\partial U}{\partial p_0}(x) \Big|_{H,M} + \frac{a_2}{h(x)} \mathcal{H}(x - x_s) \frac{\partial U}{\partial m}(x) \Big|_{H,p_0},$$

with corresponding objective function

$$I_3(x, x_s, \xi) = \int_{\xi}^{x_s} c_1 \frac{\partial p}{\partial p_0}(x) \Big|_{H,M} dx + \int_{x_s}^1 \left(\frac{a_2}{h(x)} \frac{\partial p}{\partial m}(x) \Big|_{H,p_0} + c_2 \frac{\partial p}{\partial p_0}(x) \Big|_{H,M} \right) dx - (p_2 - p_1) \delta.$$

Perturbation between the shock and the exit ($x_s < \xi < 1$)

There are now no perturbations upstream of the shock, so

$$a_1 = b_1 = c_1 = 0.$$

Perturbations in the region between the shock and ξ are denoted by a_2, b_2, c_2 and those between ξ and the exit are denoted by a_3, b_3, c_3 .

Compatibility at the shock and the fact that mh and p_0 are perturbed at constant H , together imply that there are no perturbations to stagnation enthalpy following the shock, so $b_2 = b_3 = 0$. Perturbations to the mass flux must be constant throughout the subsonic region ($a_2 = a_3 \equiv a$) since the jump condition at ξ corresponds solely to a unit perturbation in stagnation pressure

$$c_3 - c_2 = 1.$$

Zero mass flux perturbation at the shock then gives

$$a + c_2 \left(\frac{\partial m}{\partial p_0}(x) \Big|_{H,M} \right) \Big|_{x=x_s^+} = 0,$$

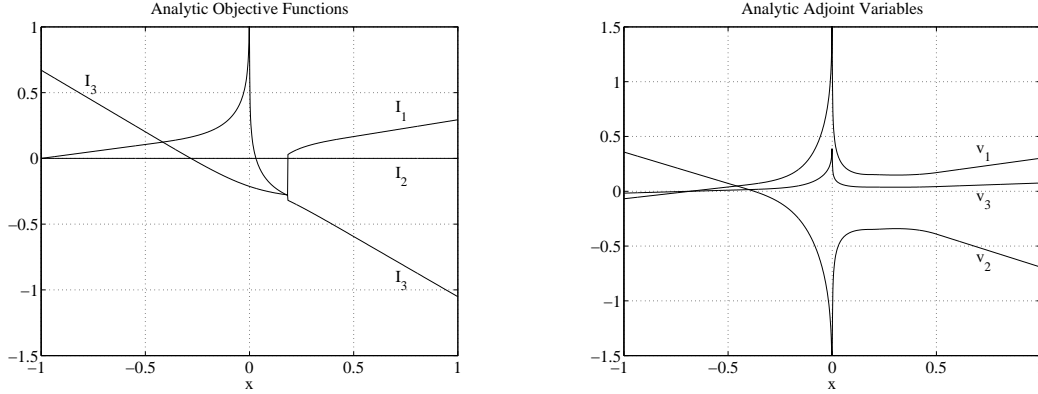


Figure 2: Objective functions and adjoint variables for shocked flow conditions.

and zero perturbation to the exit pressure requires

$$\left(\frac{a}{h(x)} \frac{\partial p}{\partial m}(x) \Big|_{H,p_0} + c_3 \frac{\partial p}{\partial p_0}(x) \Big|_{H,M} \right) \Big|_{x=1} = 0,$$

providing three equations for three unknowns. The solution has the form

$$u_3(x, x_s, \xi) = [c_2 \mathcal{H}(x - x_s) + (c_3 - c_2) \mathcal{H}(x - \xi)] \frac{\partial U}{\partial p_0}(x) \Big|_{H,M} + \frac{a}{h(x)} \mathcal{H}(x - x_s) \frac{\partial U}{\partial m}(x) \Big|_{H,p_0},$$

with corresponding objective function

$$I_3(\xi) = \int_{x_s}^1 \frac{a}{h(x)} \frac{\partial p}{\partial m}(x) \Big|_{H,p_0} dx + \int_{x_s}^{\xi} c_2 \frac{\partial p}{\partial p_0}(x) \Big|_{H,M} dx + \int_{\xi}^1 c_3 \frac{\partial p}{\partial p_0}(x) \Big|_{H,M} dx - (p_2 - p_1)\delta.$$

3.3.5 Sample solution

The objective functions $I(\xi)$ and adjoint variables $v(\xi)$ are shown in Fig. 2 for shocked flow. Again, the sonic throat produces a logarithmic singularity in the adjoint variables. At the shock, the objective functions are discontinuous but the adjoint variables are continuous with zero gradient, as proved earlier.

4 Properties of numerical solutions

The analytic adjoint solution for shocked flow is compared with first-order accurate numerical solutions computed using both the discrete and continuous formulations in Fig. 3. The internal adjoint boundary condition (2.5) is not explicitly enforced using either approach. However, both numerical solutions compare very well with the analytic results, capturing the singularity at the sonic point without oscillation, and correctly predicting continuity and zero gradients at the shock.

Some explanation is required for the correct behavior of the numerical adjoint solutions at the shock, since the internal boundary condition has not been explicitly incorporated in the discretisation. Giles has previously shown that for shocked flow [17], a second-order discretisation that degenerates to first-order accuracy at shocks still produces a second-order lift prediction. Therefore, linearisation of this discretisation should produce a linearised lift perturbation that is at least first-order accurate. Hence, we expect that the discrete adjoint

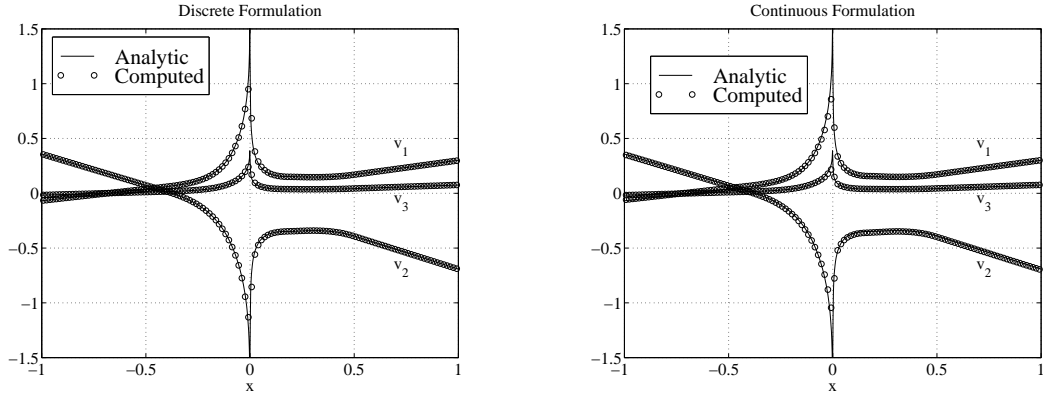


Figure 3: Adjoint solutions for shocked flow using discrete and continuous formulations

formulation, which is based on this linearised discretisation, must behave correctly to first order at the shock.

By contrast, the reason for the correct behavior of the continuous formulation is not immediately evident. Maintaining continuity at the shock, but choosing different values for the shock boundary condition leads to a one-parameter family of adjoint solutions. The effect of varying the value of the shock b.c. can be studied by modifying the value of the single outgoing characteristic variable at the exit and marching the solution upstream to the throat using a simple shooting method. Three different solutions obtained using this approach are shown in Fig. 4, where it is evident that a smooth solution is produced only when using the correct value of the shock boundary condition. This suggests that the numerical dissipation in the discretization of the continuous approach could be responsible for producing the correct adjoint behavior at the shock, since even in the absence of an explicit boundary condition, the dissipation will seek out the smoothest solution, which is also the analytic solution.

The conclusion of this analysis is that there is no clear preference for either the continuous or the discrete approach in regard to the treatment of sonic points or shocks.

5 Error analysis by adjoint methods

Previously, the adjoint flow equations were derived in the context of aerodynamic design, with a perturbation in the duct height $h(x)$ producing a perturbation to the lift. However, adjoint equations also play an important role in error analysis, predicting the error in the computed lift due to the truncation error of the numerical discretization.

Consider a discretisation of the Euler equations using first-order characteristic smooth-

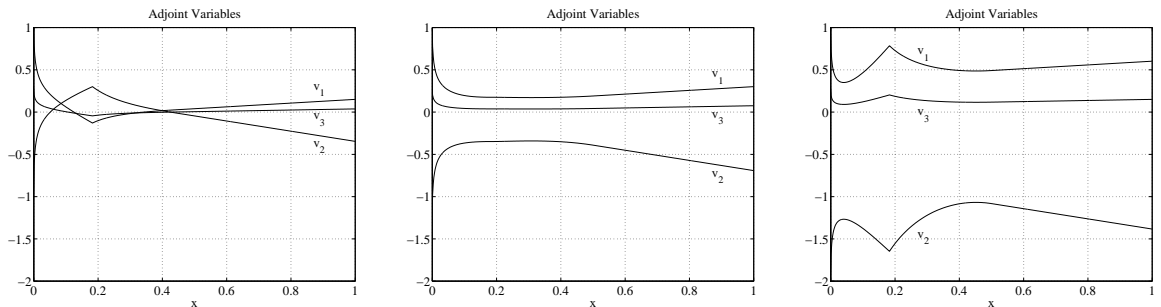


Figure 4: Adjoint solutions marched from the exit to the throat using exit b.c.'s with 0.5, 1.0 and 2.0 times the analytic value of the outgoing characteristic adjoint variable.

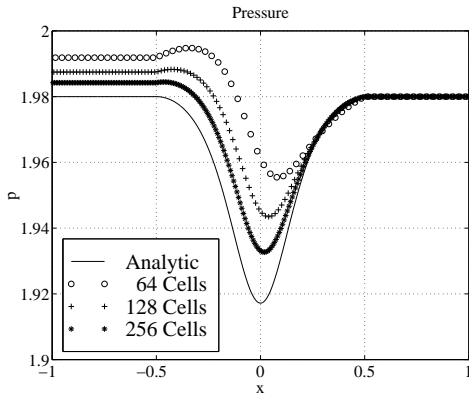


Figure 5: Pressure convergence on three meshes.

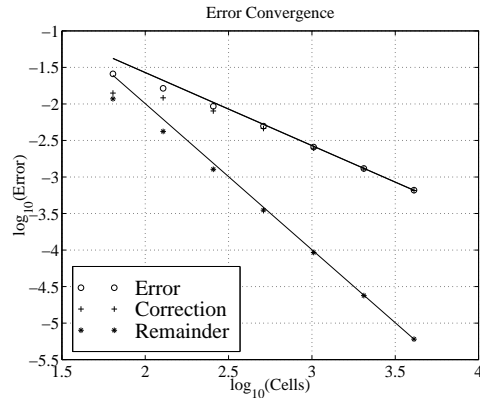


Figure 6: Convergence of the lift error, the correction and the remaining error.

ing. For simplicity, we will consider only subsonic flows for which the numerical solution U_j is smooth. Performing a modified equation analysis [18, 19] by substituting Taylor series expansions for each discrete variable results in the modified o.d.e.

$$\frac{d}{dx}(hF) - \frac{dh}{dx}P = f + O(\Delta x^2), \quad f \equiv \frac{d}{dx} \left(\frac{\Delta x}{2} h |A| \frac{dU}{dx} \right).$$

Treating the truncation error f in the same way as the design perturbation source term f in Section 2, the perturbation to the lift is once more given by (2.3), where the adjoint solution is exactly the same as before.

By evaluating this integral using computed values for the adjoint solution and truncation error, the error in the computed lift can be accurately estimated. This error estimate can then be used to correct the computed lift value. As an example, consider the subsonic test case of Fig. 5, where pressure plots are shown for three different computational grids. The first order accuracy of the discretisation results in very poor agreement with the analytic solution, which is symmetric about $x = 0$. The log-log plot of Fig. 6 displays three sets of data for meshes ranging from 64 to 4,096 cells: the error in the computed lift, the adjoint error estimate and the remaining lift error after subtracting the correction from the computed value. The superimposed lines have slopes of -1 and -2 , showing that the error and the error estimate are both first-order, as predicted, and the remaining error after applying the correction is second-order.

For higher order methods in multiple dimensions (e.g. second-order methods for Navier-Stokes calculations on unstructured 3D grids), it would be much more difficult to estimate the truncation error, and hence, to derive precise lift and drag error estimates. A more practical alternative is to use the adjoint integral error estimate (2.3) as the basis for optimal grid adaptation. Consider a local region of the grid. Doubling the grid resolution will produce a factor two reduction in the truncation error (for the first order discretisation) at the cost of introducing $O(\Delta x^{-1})$ additional grid points. Thus, the error reduction per grid point is $O(\Delta x v^T f)$. An optimal adaptation strategy is to introduce additional grid points in the regions in which $\Delta x v^T f$ is greatest. In implementing such a strategy, an accurate evaluation of the truncation error and adjoint solution is not necessary; a good order-of-magnitude estimate might be sufficient.

This optimal grid adaptation strategy looks very similar to other refinement strategies which focus on minimising the truncation error. The important distinction is the use of the adjoint solution which defines the influence of the local truncation error on the computed

quantity of most interest, such as the lift. In the shock-free transonic flow case this would focus attention on the throat region where the logarithmic singularity in the adjoint variables indicates that local truncation errors produce significant errors in the overall lift prediction.

6 Conclusions

A number of analytic and numerical properties of solutions to the quasi-1D adjoint Euler equations have been examined. Derivation of the adjoint problem for shocked flow demonstrates that the adjoint variables are continuous with zero gradient at the shock, and that a single adjoint shock b.c. is required. The analytic adjoint solution is then derived for isentropic and shocked transonic flow, revealing a logarithmic singularity at the sonic point. Numerical experiments with both the discrete and continuous adjoint formulations suggest that the adjoint solution behaves correctly at the shock without explicit enforcement of the internal boundary condition. An adjoint approach to *a posteriori* error analysis is then demonstrated and the implications for developing an optimal adaptive algorithm are discussed.

Acknowledgments

Support for this research was provided by EPSRC under grant GR/K91149.

References

- [1] A. Jameson. Aerodynamic design via control theory. *J. Sci. Comput.*, 3:233–260, 1988.
- [2] A. Jameson and J. Reuther. Control theory based airfoil design using the Euler equations. AIAA Paper 94-4272-CP, 1994.
- [3] J. Reuther, A. Jameson, J. Farmer, L. Martinelli, and D. Saunders. Aerodynamic shape optimization of complex aircraft configurations via an adjoint formulation. AIAA Paper 96-0094, 34th Aerospace Sciences Meeting and Exhibit, Reno, NV, 1996.
- [4] A. Jameson, N.A. Pierce, and L. Martinelli. Optimum aerodynamic design using the Navier–Stokes equations. AIAA Paper 97-0101, 35th Aerospace Sciences Meeting, Reno, NV. (*J. Theor. Comput. Fluid Mech.*, to appear), 1997.
- [5] O. Baysal and M.E. Eleshaky. Aerodynamic sensitivity analysis methods for the compressible Euler equations. *J. Fluids Engng*, 113:681–688, 1991.
- [6] S. Ta’asan, G. Kuruvila, and M.D. Salas. Aerodynamic design and optimization in one shot. AIAA Paper 92-0025, 1992.
- [7] J. Elliot and J. Peraire. Aerodynamic design using unstructured meshes. AIAA Paper 96-1941, 1996.
- [8] W.K. Anderson and V. Venkatakrisnan. Aerodynamic design optimization on unstructured grids with a continuous adjoint formulation. AIAA Paper 97-0643, 1997.
- [9] C. Johnson and R. Rannacher. On error control in computational fluid dynamics. Technical Report 94-13, Universitat Heidelberg, 1994.
- [10] R. Becker and R. Rannacher. Weighted *a posteriori* error control in finite element methods. Technical Report 96-1, Universitat Heidelberg, 1996.

- [11] E. Süli and P. Houston. Finite element methods for hyperbolic problems: *a posteriori* error analysis and adaptivity. In I.S. Duff and G.A. Watson, editors, *State of the Art in Numerical Analysis*. Oxford University Press, 1996.
- [12] M.B. Giles. On adjoint equations for error analysis and optimal grid adaptation in CFD. Technical Report 97/11, Oxford University, 1997. Presented at Computing the Future II: Advances and Prospects in Computational Aerodynamics.
- [13] M.B. Giles and N.A. Pierce. Adjoint equations in CFD: duality, boundary conditions and solution behavior. AIAA Paper 97-1850, 1997.
- [14] A. Iollo, M.D. Salas, and S. Ta'asan. Shape optimization governed by the Euler equations using an adjoint method. ICASE Report No. 93-78, 1993.
- [15] A. Iollo and M.D. Salas. Contribution to the optimal shape design of two-dimensional internal flows with embedded shocks. *J. Comput. Phys.*, 125:124–134, 1996.
- [16] E.M. Cliff, M. Heinkenschloss, and A.R. Shenoy. On the optimality system for a 1-D Euler flow problem. AIAA Paper 96-3993-CP, 1996.
- [17] M.B. Giles. Analysis of the accuracy of shock-capturing in the steady quasi-1D Euler equations. *Comput. Fluid Dyn. J.*, 5(2):247–258, 1996.
- [18] R. Warming and Hyett. The modified equation approach to the stability and accuracy analysis of finite-difference methods. *J. Comput Phys*, 14:159–179, 1974.
- [19] R.J. LeVeque. *Numerical Methods for Conservation Laws*. Birkhauser Verlag, 1992.